Inelastic Design and Testing of Steel Bridges Comprising Noncompact Sections

BRYAN A. HARTNAGEL and MICHAEL G. BARKER

INTRODUCTION

Inelastic design procedures allow the designer flexibility and the possibility of more economical designs by decreasing member sizes and eliminating cover plates and flange transitions at negative moment regions. Previous experimental results show that compact girders designed by these procedures perform satisfactorily when subject to design load levels.

Current provisions, however, apply only to compact steel bridges. Expanding inelastic design provisions to include noncompact sections is desirable because of the wide use of plate girders with thinner webs. General inelastic provisions applicable to compact and noncompact sections will create designs that are more consistent over the steel bridge inventory. Previous research has shown that noncompact girders have predictable moment-rotation behavior that can be incorporated into inelastic design provisions. However, although the analytical tools exist, large-scale testing is necessary to validate theoretical engineering practice.

Inelastic steel bridge design procedures account for the reserve strength inherent in multiple-span steel girder bridges by allowing redistribution of negative pier region elastic moments to adjacent positive moment regions. The redistribution causes a slight inelastic rotation at the interior pier sections, residual moments in the beam, and some permanent residual deflection. After the redistribution, the structure achieves shakedown: deformations stabilize and future loads are resisted elastically.

Comprehensive inelastic design procedures were first permitted for highway bridges with the adoption of guide specifications for Alternate Load Factor Design (ALFD) in 1986 (AASHTO, 1991). These design procedures, originally called autostress design procedures, are applicable only to compact sections. The procedures specify a strength check by the plastic-design mechanism method at Maximum Load and a permanent-deflection check by the beam-line method at Overload. In this latter check, yielding is allowed to occur at peak negative-moment locations (piers) and the resulting redistribution moments (automoments) are calculated. The stresses in positive-bending regions after redistribution are limited to 95 percent and 80 percent of the yield stress at composite and noncomposite sections, respectively. These same stress limits are imposed at both the positive- and negative-bending sections in the 1996 LFD specifications (AASHTO, 1996) and are assumed to prevent objectionable permanent deflections. In 1994, the inelastic design procedures from the ALFD guide specifications (AASHTO, 1991) were incorporated into the new AASHTO Load and Resistance Factor Design (LRFD) bridge specifications (AASHTO, 1998) with minor modifications and additions. New provisions that include inelastic design of noncompact sections were proposed to the American Iron and Steel Institute (AISI) in February 1997 (Schilling, Barker, Dishongh, and Hartnagel, 1997).

A one-third-scale bridge girder was subjected to modeled LRFD design loads. The girder was designed according to LRFD inelastic design provisions that are proposed to eventually replace Section 6.10.10 of the current LRFD inelastic design specifications. Three primary changes are proposed. The first is a relaxation of web slenderness limits to allow the use of noncompact sections. The second allows the use of a noncompact moment-rotation model for the pier section. Finally, a ϕ factor is added similar to those specified in LRFD Section 6.5.4.2 to be applied to the maximum load shakedown limit. The objectives of this paper are to present experimental verification for inelastic design of bridges comprising noncompact sections and present the new proposed procedures.

PROPOSED LRFD INELASTIC DESIGN PROCEDURES

Current LRFD design provisions do not allow inelastic design methods to be used with noncompact cross-sections. One of the objectives of the research is to allow the use of cross sections that have noncompact webs. The proposed design specifications will be briefly presented herein. A full discus-

Bryan A. Hartnagel is assistant professor, Colorado State University, department of civil engineering, Fort Collins, CO.

Michael G. Barker is associate professor, University of Missouri-Columbia, department of civil and environmental engineering, Columbia, MO.

sion and justification can be found in Schilling et al. (1997) and Hartnagel (1997).

The proposed LRFD inelastic design procedures limit the compression flange slenderness to:

$$\frac{b_f}{2t_f} \leq 0.408 \sqrt{\frac{E}{F_{yc}}} \tag{1}$$

and web slenderness is limited to:

$$\frac{2D_c}{t_w} \leq 6.77 \sqrt{\frac{E}{F_{yc}}} \tag{2}$$

The proposed procedures are limited to steel with a specified minimum yield strength not exceeding 345 MPa (50 ksi). The loading and limit states are the same as for the current LRFD provisions (AASHTO, 1998).

Design Limit States

Fatigue and Fracture Limit State

The standard design truck is assumed for the Fatigue and Fracture Limit State. However, the rear axle spacing is a constant 9.14 m (30 ft). The load factor for the live load is 0.75. A 15 percent dynamic load allowance is applied to the live load vehicle.

Service Limit State Control of Permanent Deflections

The Service Limit State is intended to prevent permanent deformations due to localized yielding. This design limit uses the Service II Load Combination. The Service II Load Combination is $DC + DW + 1.3L(1+I)$. For the proposed LRFD inelastic design provisions, positive moment stresses are limited to 95 percent F_y for composite sections and to 80 percent F_y for noncomposite sections after redistribution of the interior support moment. The elastic stress at any location is the sum of the stresses caused by the loads applied separately to: the steel (DC_1), the short-term composite section (L), and the long-term composite section (DW and DC_2) (AASHTO, 1998). There is no stress limit at the interior support regions. The redistribution moment, M_{rd}, at each interior support is shown below:

$$M_{rd} = M_{pe} - M_e \geq 0 \tag{3}$$

where

$M_{pe} = M_p$ for flanges satisfying $\frac{b_f}{2t_f} \leq 0.291 \sqrt{\frac{E}{F_{yc}}}$ or

compact sections satisfying both

$$\frac{2D_{cp}}{t_w} \leq 3.76 \sqrt{\frac{E}{F_{yc}}}$$

and

$$\frac{b_f}{2t_f} \leq 0.382 \sqrt{\frac{E}{F_{yc}}}$$

$M_{pe} = 0.8R_hM_y$ for all other sections

M_e = elastic moment at the interior support due to the factored loading

R_h = hybrid flange-stress reduction factor specified in Article 6.10.4.3.1.

At all other locations, the redistribution moment is determined by connecting the moments at interior supports by straight lines and extending these lines from the first and last interior supports to points of zero moments at adjacent abutments. This ensures a self-equilibrating residual moment field.

Strength Limit State

The proposed simplified Strength Limit State is a shakedown limit state. The Strength I Load Combination is used for this design check. As an alternate to the proposed shakedown limit state, Schilling's unified autostress method (Schilling, 1991; Schilling, 1993) or the residual deformation method by Dishongh and Galambos (1992) are allowable methods of inelastic analysis for bridges.

For the shakedown check, the flexural resistance of all sections shall satisfy:

$$M_r = \phi_{sd} \, M_{pe} - M_{rd} \tag{4}$$

where

ϕ_{sd} = resistance factor for shakedown (= 1.1)

M_{pe} = effective plastic moment capacity (shown below)

The redistribution moment at each of the interior supports is taken as:

$$M_{rd} = \phi_{sd} \, M_{pe} - M_e \geq 0 \tag{5}$$

where

M_e = elastic moment at interior support due to the factored loading

At all other sections, the redistribution moment diagram shall be determined by connecting the moments at all interior supports with straight lines and extending these lines from the first and last interior supports to points of zero moment at the adjacent abutments. The effective plastic moment at the interior supports is determined as follows depending on the compression flange slenderness and the web slenderness. For sections that satisfy:

$$\frac{b_f}{2t_f} \leq 0.291 \sqrt{\frac{E}{F_{yc}}} \tag{6}$$

If $\frac{2D_{cp}}{t_w} \leq 3.76\sqrt{\frac{E}{F_{yc}}}$, then:

$$M_{pe} = M_p \tag{7}$$

If $3.76\sqrt{\frac{E}{F_{yc}}} < \frac{2D_{cp}}{t_w} \leq 5.05\sqrt{\frac{E}{F_{yc}}}$, then:

$$M_{pe} = R_h M_y \tag{8}$$

If $\frac{2D_{cp}}{t_w} > 5.05\sqrt{\frac{E}{F_{yc}}}$, then:

$$M_{pe} = \left[1.56 - 0.111\left(\frac{2D_{cp}}{t_w}\right)\sqrt{\frac{F_{yc}}{E}}\right] R_h M_y \tag{9}$$

where

b_f = compression flange width

t_f = compression flange thickness

D_{cp} = depth of web in compression at the plastic moment specified in Article 6.10.3.1.4b or 6.10.3.3.2

t_w = web thickness

F_{yc} = specified minimum yield strength of the compression flange

M_y = yield moment specified in Article 6.10.3.1.2 or 6.10.3.3.1

M_p = plastic moment specified in Article 6.10.3.1.3 or 6.10.3.3.1

M_{pe} = Strength Limit State effective plastic moment, and

R_h = hybrid flange-stress reduction factor specified in Article 6.10.4.3.1

If the effective plastic moment is determined from any of the three Equations (7-9) above, a transverse stiffener must be placed a distance of one-half the web depth on each side of that support. Tests have shown that girders with ultra-compact compression flanges satisfying Equation 6, and with transverse stiffeners near the peak-moment location, provide good rotation characteristics even if the web is noncompact (Schilling and Morcos, 1988). If the cross section has flanges that are compact but not ultra-compact then the effective plastic moment capacity is calculated using the effective yield strengths presented in LRFD Article 6.10.10.1.2d.

COMPARISON TO ELASTIC METHODS

A prototype bridge with noncompact sections was designed using the proposed inelastic design provisions. The prototype design is presented in the next section. Load ratings of this girder using the current design methods available for noncompact girders are presented in Table 1. The Service Limit State Control of Permanent Deflection controlled for the proposed LRFD inelastic design, but the Strength Limit State (Maximum Load for LFD) controlled for the remaining methods. Current bridge specifications do not allow for inelastic design or redistribution of negative pier moments for bridges comprising noncompact sections.

Table 1. Comparison of Design Methods

Design Method	Design Load
Current LRFD Inelastic Design	Not Applicable
LFD Elastic No Redistribution	HS6.4
LRFD Elastic No Redistribution	HS5.2
Proposed LRFD Inelastic Design	HS20

The elastic design provisions (LFD and LRFD) have much lower load ratings for the prototype girder than the proposed LRFD inelastic design provision. Inelastic design provisions for noncompact sections should have significantly higher load ratings than bridges that are forced to remain elastic at factored loads. However, this large difference in design load is partly because this girder had very high dead load stresses. The available stress remaining for live load is small and, when the total stress must remain elastic, the live load capacity is low.

TWO-SPAN COMPOSITE GIRDER TEST

Prototype Bridge Design

A bridge with noncompact girder sections was designed using the proposed simplified inelastic design provisions. The bridge is a two-span structure with span lengths of 50.3 m-50.3 m (165 ft-165 ft). A 12.8 m (42-ft) wide deck was supported by four plate girders with a spacing of 3.66 m (12 ft). Figure 1 shows a cross section of the prototype bridge. A specified minimum yield strength of 345 MPa (50 ksi) is assumed and the 28-day compressive strength of the 229 mm (9 in.) thick concrete deck is 27.5 MPa (4,000 psi). Dead and live loadings are in accordance with the current AASHTO LRFD Specifications (AASHTO, 1998). A 575 Pa (12 psf) future wearing surface and two 4.45 kN/m (305-plf) barriers are also applied to the bridge. A single-lane ADTT of 540 is assumed for the fatigue design.

Two different cross sections were assumed along the length of the girder. One cross section was assumed for the interior support region and another was assumed for the positive moment region. Both sections are 1,753 mm (69-in.) deep plate girders. Cross section geometry of the two regions is shown in Figure 2. The interior support region extends 10.05

Table 2. Prototype and Model Girder Section Properties[a]					
Property	Scale Factor	Prototype		Model	
Non-Composite		Midspan	Pier	Midspan	Pier
I_x (mm^4)*10^6	1/81	21,600	31,900	267	395
S_t (mm^3)*10^6	1/27	21.5	31.3	0.803	1.16
S_b (mm^3)*10^6	1/27	27.2	40.1	1.02	1.49
Composite n=8					
I_x (mm^4)*10^6	1/81	58,400	42,900	720	529
S_b (mm^3)*10^6	1/27	38.5	44.6	1.43	1.64
Composite n=24					
I_x (mm^4)*10^6	1/81	43,200		533	
S_b (mm^3)*10^6	1/27	35.4		1.31	
Plastic Moment					
M_p (kN-m)	1/27	17,350	17,350	643	643
M_{pe} (kN-m)	1/27		14,240		527

[a] 1 mm = 0.03937 in, 1 kN-m = 0.7376 k-ft.

m (33 ft) on either side of the pier. Figure 2 also illustrates the prototype girder elevation. The girder is designed as a single interior girder with live load effects approximated assuming the current LRFD live load distribution factors (AASHTO, 1998). Cross sectional properties of the negative and positive moment regions are shown in Table 2.

Loads

The dead load of the steel girder and the concrete deck, component dead load DC_1, is applied to the noncomposite section. Moments from the component dead load, DC_1, are 3,990 kN-m (2,940 k-ft) for the positive moment region and −8,420 kN-m (−6,210 k-ft) for the interior support. The weight of the barrier curbs, DC_2, is applied to the long-term composite section. These moments are 396 kN-m (293 k-ft) and −709 kN-m (−524 k-ft) respectively for the positive and negative moment regions. Moments for the future wearing surface, DW, are 373 kN-m (277 k-ft) for the positive moment region and −671 kN-m (−496 k-ft) for the interior support. Weight of the future wearing surface, DW, is applied to the long-term composite section.

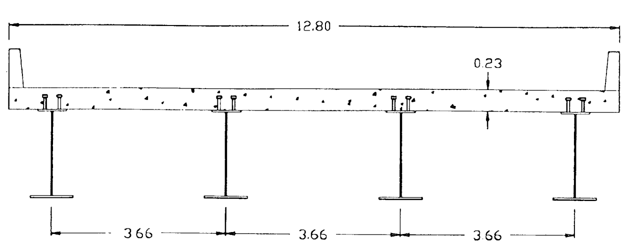

Fig. 1. Prototype bridge cross section.

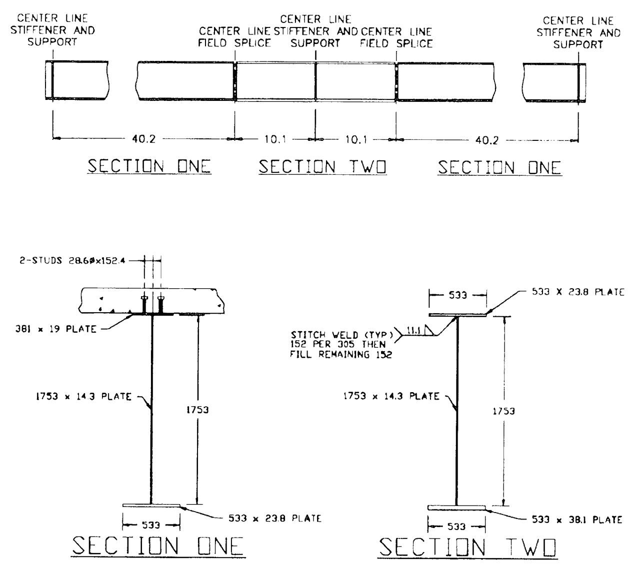

Fig. 2. Prototype girder elevation and cross sections.

Live loads and impact are applied to the short-term composite section in the positive moment region. At the interior support, the structural resistance is the steel section plus the contribution of the longitudinal reinforcing steel in the concrete deck within the effective width. All moments were computed using a non-prismatic elastic analysis. Appropriate cross sections were used to determine the effects of the various loadings. Positive moments were based on the LRFD HL-93 loading (AASHTO, 1998) that consists of a 9.34 kN/m (640 plf) lane load and a HS20 truck with 33 percent impact included only on the truck. Negative moments were based on 90 percent of both the lane load and two HS20 trucks spaced 15.24 m (50 ft) apart from front to rear with impact included only on the trucks (LRFD Article 3.6.1.2). Factored live load moments for the girder were 4,810 kN-m (3,550 k-ft) for the positive moment region and –3,950 kN-m (–2,910 k-ft) for the interior support region. Dead and live load girder moments are shown in Figure 3.

Design Limit States

Service Limit State Control of Permanent Deflection

For the girder under consideration, the Service Limit State Control of Permanent Deflection is satisfied as evidenced by the following calculations.

In Equation 3, M_e is calculated as:

$$M_e = -9{,}129 - 671 + 1.3(-3{,}950) = -14{,}940 \text{ kN–m} \quad (10)$$

For sections that satisfy the ultra-compact compression flange requirements of the proposed provisions:

$$M_{pe} = M_p = -17{,}350 \text{ kN–m} \quad (11)$$

The redistribution moment, M_{rd}, is calculated from Equation 3:

$$M_{rd} = M_{pe} - M_e = -17{,}350 - (-14{,}940)$$
$$= -2{,}420 \text{ kN–m} \geq 0 \quad (12)$$

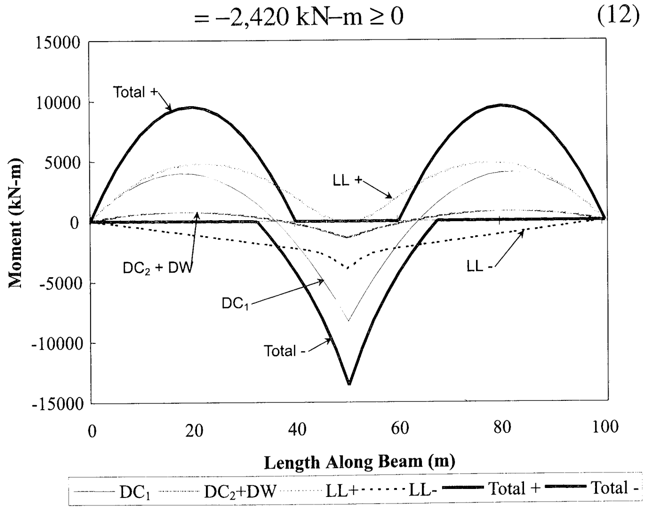

Fig. 3. Moment envelopes for the prototype girder.

Because the effective plastic moment capacity is greater than the elastic moment demand for the Service II Load Combination, there is no redistribution moment. The limit state check is a limited stress in the positive moment region. For composite sections, the stress is limited to 95 percent of F_y. The design check is demonstrated below using properties from Table 1:

$$\frac{3{,}990}{0.0272} + \frac{770}{0.0354} + \frac{1.3(4{,}810)}{0.0385} = 331 \text{ MPa}$$
$$\approx 327 \text{ MPa} \checkmark \text{ ok} \quad (13)$$

The Service Limit State is satisfied. This limit state is intended to prevent objectionable permanent deflections due to an occasional overload.

Strength Limit State

The following calculations show the girder satisfies the proposed simplified inelastic design Strength Limit State. The proposed inelastic design provisions require a transverse stiffener be placed a distance of one-half the web depth on each side of the support. However, these stiffeners were omitted from the test girder. Previous research has shown that the transverse stiffeners enhance the moment-rotation behavior of the cross section (Schilling and Morcos, 1988). It was decided to determine if the girder could perform satisfactorily without the stiffeners. If so, the girder would perform even better with the stiffeners. For the Strength Limit State loading, the resistance of any cross section is determined from Equation 4 and the effective plastic moment capacity, M_{pe}, is determined from the above Equations (7-9). The interior support resistance is calculated below.

$$M_r = 1.1(-14{,}240) - M_{rd} \quad (14)$$

$$M_{rd} = 1.1(-14{,}240) - M_e \quad (15)$$

and

$$M_e = 1.25(-9{,}129) + 1.5(-671) + 1.75(-3{,}950)$$

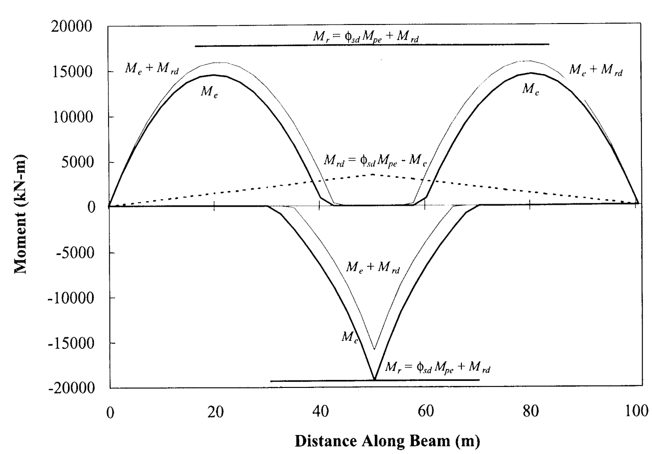

Fig. 4. Strength limit state moments.

$$= -19{,}330 \text{ kN–m} \quad (16)$$

Calculating M_{rd} and M_r as follows:

$$M_{rd} = 1.1(-14{,}240) - (-19{,}330) = 3{,}670 \text{ kN–m} \quad (17)$$

$$M_r = 1.1(-14{,}240) - 3{,}670 = -19{,}330 \text{ kN–m} \quad (18)$$

Once the interior support resistance is calculated, a design check is made to ensure the positive moment region elastic demand is less than the positive moment region resistance. The same Equation 4 is used to compute the resistance with the attributed redistribution moment, M_{rd}. Figure 4 illustrates the total and residual moments and the design capacities at the Strength Limit State design check. For the positive moment region:

$$M_r = 1.1(17{,}350) - 0.4(3{,}670) = 17{,}620 \text{ kN–m} \quad (19)$$

The elastic moment demand on the positive moment region is computed as:

$$M_e = 1.25(4{,}386) + 1.5(373) + 1.75(4{,}810)$$

$$= 14{,}460 \text{ kN–m} \leq 17{,}620 \text{ kN–m} \quad (20)$$

Therefore, the girder satisfies the Strength Limit State.

Test Procedure

An interior girder from the bridge designed by the proposed LRFD inelastic provisions was used as a prototype for the test specimen. The test girder was a one-third-scale model of the prototype bridge. Two 16.76 m (55-ft) spans were used in the model. The plate girder was designed with length increments divisible by three to accommodate the ease of scaling. Figure 2 shows the prototype girder geometry. Test section geometry can be determined by dividing each length by 3. The properties of the model are presented in Table 1.

Tension tests were performed on full thickness samples taken from the plate used to fabricate the model girder and components. The static yield strengths for the plates that make up the interior support section are well below 345 MPa (50 ksi). The bottom flange of the positive moment region and the top flange of the interior support region were made from the same plate and have an average yield strength of 290 MPa (42 ksi). The bottom flange of the interior support has an average yield strength of 269 MPa (39 ksi). The web plate for the interior support and the positive moment region has an average yield strength of 345 MPa (50 ksi). The top flange of the positive moment region had an average yield strength of 331 MPa (48 ksi).

To account for the difference between the experimental yield strength and the design yield strength; live load moments are reduced to match limit state behavior (Hartnagel, 1997). Because the dead loads on the girder are the same, there is less reserve strength to carry live loads when the yield strength of the material is lower. The Service Limit State Control of Permanent Deflection controlled the design of the prototype. The design check for this limit state is a limited stress at the positive moment region. Dead load causes the same stress in the positive moment region no matter what yield strength material is assumed. Therefore, if a lower yield strength material is assumed, a smaller live load will be allowed to meet the limit state. Live load levels were adjusted by a factor equal to the live load moment at limit state for 345 MPa (50 ksi) steel divided by the live load moment at limit state for 290 MPa (42 ksi) steel. To meet the limit state behavior, it is analogous to designing the bridge with a smaller design truck.

Test Setup

The one-third-scale model weighed only 1/9 of the prototype girder. In order to properly scale the dead load stresses in the girder, an additional amount of dead load equal to 2/9 of the weight of the prototype was placed on the girder. Concrete blocks were hung from the model before the effective width deck was placed to simulate the noncomposite dead load. Steel plates were placed on top of the concrete deck several days after placing the concrete to represent the composite dead load. Moments from the compensatory dead loads and the theoretical model dead loads are shown in Figure 5. Bracing for the girder was provided at the load points shown in Figure 6 and at 1.22 m (4 ft) and 2.44 m (8 ft) on each side of the interior support.

Twenty-eight days after placing the concrete composite deck, the live load testing began. Four hydraulic actuators were used to simulate the live load on the girder. Two were used in each span of the two-span structure as shown in Figure 6. The live load moment envelope and the modeled moment envelope are shown in Figure 5. The live loading could be applied in any level as a percentage of a Service I Live Load. The loading sequence consisted of three steps; each followed by an unloading step. Each step was designed to produce maximum moment in a specified portion of the girder. The three load steps are described below. First, actuators P1 and P2 produced maximum positive moment in the first span. Next, actuators P2 and P3 were loaded to produce maximum negative moment over the interior support. Finally, actuators P3 and P4 were loaded to produce maximum positive moment in the second span.

Load levels started at 15.4 percent of a design truck and progressed through the following levels: 15.4, 30.8, 61.5, 92.3, 107.7, 123, 138.5, 153.8, 169.2, 184.6, 200, 215.4, 238.5, 255.4, and 269. At the 269 percent load level, additional load was added with the four actuators to simulate the Strength I load factors of 1.25 *DC* and 1.5 *DW*. After the additional load was applied to simulate the additional factored dead load, the 269 percent truck was started on the bridge. With actuators P1 and P2 loaded, the first span suffered significant damage. Loading then progressed to actuators P2 and P3. At this point a large buckle in the web at the interior support occurred. The flange at the interior support also had a small buckle after actuators P2 and P3 were loaded. When the loading progressed to actuators P3 and P4, the girder continued deflecting until actuator P4 ran out of travel.

Many different measurements were taken during the testing of the model girder. Rotation measurements were made at 1.22 m (4 ft) from each end of the girder and 1.83 m (6 ft) on either side of the interior support. Strain measurements were made at four locations on the girder. At each of the strain measurement locations, ten strain gages were used on the steel cross section. Six of the gages were attached to the web of the girder. The other four gages were attached to the top and bottom flange, two gages for each flange. A 890 kN (200 kip) load cell measured the reaction at each of the three supports and 534 kN (120 kip) load cells measured the applied load at each hydraulic actuator. The interior bearing was a pin support and the end bearings were rocker supports. Figure 6 shows the layout of the measurement locations.

Test Results

Test results are summarized here for brevity. For more detailed explanation of the model behavior at all load levels, the reader is referred to Hartnagel (1997).

Fatigue and Fracture Limit State Behavior

The critical fatigue detail was the weld of the composite studs to the top flange of the girder. For this Category C fatigue check, a special fatigue vehicle is used (AASHTO, 1998). It is a HS20 truck with a 9.14 m (30 ft) spacing between the 142 kN (32 kip) axles and a dynamic load allowance of 15 percent. The allowable fatigue stress range on the composite studs was determined to be 40.2 MPa (5.83 ksi) using LRFD 6.6.1.2.5-1 (AASHTO, 1998). Assuming an elastic modulus of 200 GPa (29,000 ksi), the fatigue stress range is approximately 200 $\mu\varepsilon$. Factored measured live load strain ranges in the two-span girder at the Fatigue Limit State were 173 $\mu\varepsilon$ and 154 $\mu\varepsilon$ for gage sections two and three respectively. Therefore, the stress ranges experienced by the girder met the Fatigue and Fracture Limit State. The girder did not experience the number of fatigue cycles expected for the design, as fatigue was not the major focus of the study.

Service Limit State Behavior

The live load deflection of the girder under the Service I Load Combination was 22.6 mm (0.89 in.). As a function of span length, this is L/743. At this load level, no visible cracking of the concrete deck had occurred.

Service Limit State Control of Permanent Deflections Behavior

The 138.4 percent load level is used to check the behavior at the Service Limit State Control of Permanent Deflections. The strains are reduced by 0.93 (130/138.4), but the deformations are checked for the full 138.4 percent of the modeled truck load. At the Service Limit State, design calculations limit the positive moment region stresses to $0.95F_y$ after the redistribution of moments. For this girder, there were no design-redistributed moments due to pier yielding. The calculated stress at the positive moment region (Section 1) was 275 MPa (39.9 ksi). The allowable stress is also 275 MPa (39.9 ksi) ($0.95F_y$), resulting in an allowable strain of 1,380 $\mu\varepsilon$. The maximum measured elastic strain at the Service Limit State was 1,380 $\mu\varepsilon$ (835 $\mu\varepsilon$ dead load and 545 $\mu\varepsilon$ live load). The total measured experimental strain was 1,550 $\mu\varepsilon$. The difference between the measured elastic and total strains is due to locked in redistributed moments. Although measured total strains exceed Service II limits, the difference is small and elastic strains are within 0.95 F_y.

The proposed LRFD inelastic design provisions used to design this girder do not require a deflection check at the Service Limit State Control of Permanent Deflections. How-

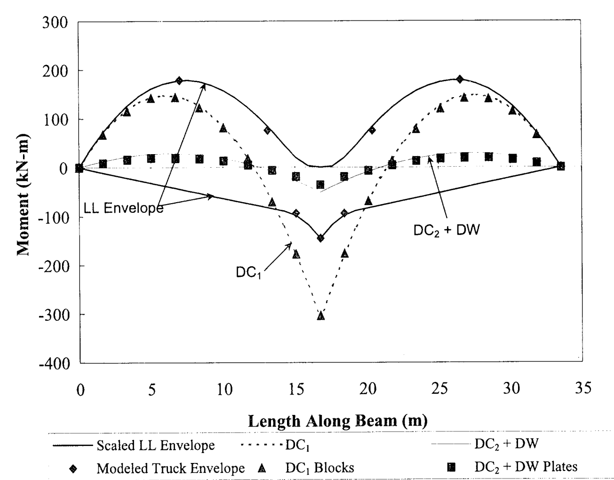

Fig. 5. Theoretical and actual dead and live load model moment diagrams.

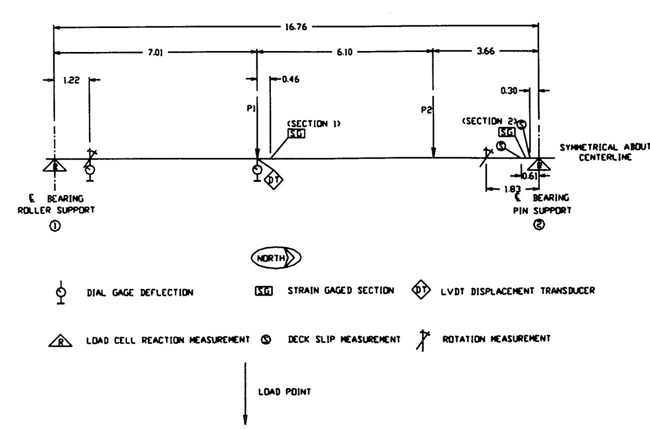

Fig. 6. Test measurement layout.

ever, the proposed provisions do refer the reader to methods to determine these deflections.

After three cycles at the 138.4 percent load level, the permanent set at Section 1 stabilized at 5.59 mm (0.22 in.). The concrete deck had visible cracking after three cycles of the 138.4 percent load level. The measured inelastic rotation at the pier was 4.7 mrads and at the positive moment region it was 2.7 mrads. Using a conjugate beam analysis, the calculated residual moment at the pier was 30 kN-m (22 k-ft) and the calculated permanent set at Section 1 was 4.58 mm (0.18 in.). These compare well to the measured residual moment at the pier of 20.3 kN-m (15 k-ft) and a measured permanent set at Section 1 of 5.59 mm (0.22 in.).

Strength Behavior

The proposed provisions use the shakedown capacity at the Strength Limit State. The design procedures are greatly simplified compared to a mechanism check.

The Strength I limit load is $1.25DC+1.50DW+1.75L(1+I)$. This is represented by the 184.6 percent load level: 175 percent plus additional factored dead load. The requirement is that the structure shakes down at this load. Figure 7 shows the residual permanent set after eight cycles of this loading for the girder. Shakedown is demonstrated by stabilization of permanent deflections after each cycle. As can be seen, the girder definitely shakes down at the 184.6 percent level. In fact, the girder achieved shakedown at load levels well above the Strength I Load Combination. This is expected since the Strength Limit State did not control the design.

The moment-inelastic rotation curve at the negative pier section is important for determining the Strength Limit State design capacity. The ability of the noncompact girder sections to maintain a reliable moment capacity during sufficient inelastic rotations is essential for the redistribution of moments. Figure 8 shows the moment-inelastic rotation for the pier section during the cyclic tests. At the Strength Limit State, the measured moment was 560 kN-m (413 k-ft) at a measured inelastic rotation of 8 mrads. This corresponds to a calculated design moment of M_{pe} = 431 kN-m (318 k-ft). The maximum usable moment according to the proposed design provisions is M_{pe} where M_{pe} equals 576 kN-m (425 k-ft) for the Service Limit State Control of Permanent Deflections check and 431 kN-m (318 k-ft) for the Strength Limit State check. The beam surpassed these levels.

Examining the theoretical shakedown limit (the maximum Strength Limit State) at the 255.3 percent level, the measured pier moment was 622 kN-m (459 k-ft) at an inelastic rotation of 9.6 mrads, which exceeds the proposed Strength Limit State moment capacity of M_{pe} = 431 kN-m (318 k-ft). The pier section was able to retain more moment than expected. It is possible that this is due to strain hardening of the steel. At the positive section, the measured moment was 454 kN-m (335 k-ft) while the theoretical moment was 542 kN-m (400 k-ft) assuming the pier section shed moment. This illustrates reserve strength that is inherent in continuous steel girders.

SUMMARY

Inelastic steel bridge design procedures account for the reserve strength inherent in multiple-span steel girder bridges by allowing redistribution of negative pier region elastic moments to adjacent positive moment regions. The redistribution causes slight inelastic rotation at the interior pier sections, residual moments in the beam, and some permanent residual deflection. After the redistribution, the structure achieves shakedown: deformations stabilize and future loads are resisted elastically.

The objectives of the research project were to:

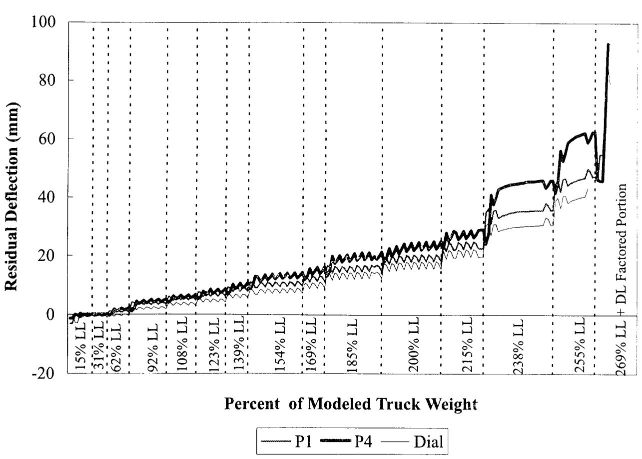

Fig. 7. Residual deflection vs percent of modeled truck weight.

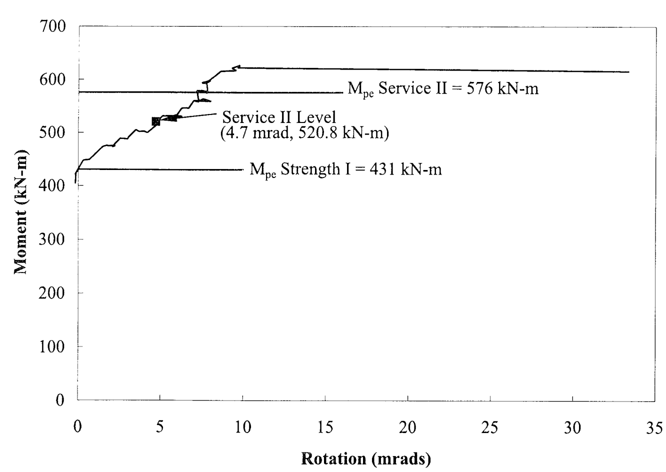

Fig. 8. Moment vs inelastic-rotation for the interior support.

1. Propose new comprehensive and practical inelastic design procedures that allow compact and noncompact sections, presented in detail in Schilling et al. (1997),
2. Experimentally verify inelastic limit state behavior with a one-third scale continuous span test of a composite girder, and
3. Examine the moment-rotation behavior of compact and noncompact pier sections.

The one-third scale two-span continuous composite girder was subjected to an (adjusted) simulated moving HS20 loading. The girder was designed and modeled to represent an interior girder of a proposed LRFD inelastic design prototype.

During simulated moving load tests, the girder suffered plastic collapse above the shakedown load. Below is a summary of the findings during the experimental program.

The model behaved according to elastic structural theory. The elastic deflections and stresses (strains) were in reasonable agreement to those predicted. The measured Service II Load Combination stresses (strains) nearly met (within 12 percent) the Service Limit State Control of Permanent Deflections criteria. Residual deflections stabilized after three cycles of the Service II Load Combination. This bridge was a very efficient design where both the pier and positive moment region were at design limits. The fatigue stresses met design criteria. The noncompact pier section redistributed moments and measured permanent residual deflections were approximately equal to the predicted moments and deflections. The simplified proposed LRFD inelastic design procedures do not require the determination of deflections. However, the current and proposed LRFD inelastic design provisions refer the engineer to methods of determining deformations if deemed important.

The experimental moment at the Service Limit State Control of Permanent Deflection and Strength levels exceeded moments predicted by the design provisions. The proposed LRFD inelastic design provisions use an effective plastic moment capacity, M_{pe}, at each limit state and there is no need to relate moment to inelastic rotation. M_{pe} depends on the web and flange slenderness ratios. The girder obtained shakedown above the theoretical incremental collapse level. The pier section maintained higher than predicted moments at large rotations. The last cycle of loads that caused the girder to collapse was well above theoretical collapse load.

The proposed LRFD inelastic design procedures allow the use of compact and noncompact girder sections. The proposed LRFD inelastic design provisions are also greatly simplified compared to current inelastic design methods. The provisions are no more difficult to apply than the LFD or LRFD elastic provisions that allow 10 percent redistribution of pier moments if the pier sections are compact. The tests performed in this project support the development and verify the procedures of the proposed inelastic design provisions for bridges comprising noncompact girders. The limit state design levels were satisfied and the overall behavior of the girders was satisfactory.

IMPACT OF PROPOSED LRFD INELASTIC DESIGN PROVISIONS

Inelastic design procedures, currently limited to bridges comprising compact sections, offer the potential for significant cost savings by accounting for a better estimate of the true strength and behavior of the bridge. Also, inelastic techniques permit greater design flexibility such as optimizing material use by eliminating cover plates and flange transitions, and quantifying the redistribution characteristics for more consistent safety considerations. The proposed provisions allow the use of compact and noncompact girder sections, unlike current procedures that are limited to compact sections. The proposed LRFD inelastic design provisions are also greatly simplified compared to current inelastic design methods.

ACKNOWLEDGMENTS

The authors gratefully acknowledge the sponsors of this work: the National Science Foundation, the American Iron and Steel Institute, the American Institute of Steel Construction, Missouri Department of Transportation, Louisiana Transportation Research Center, Bethlehem Steel, Nucor-Yamato Steel, U.S. Steel, St. Louis Screw and Bolt Co., Stupp Bros. Inc., and Delong's Inc.

REFERENCES

AASHTO (1991), *Guide Specifications for Alternate Load Factor Design Procedures for Steel Beam Bridges Using Braced Compact Sections*, Washington, D.C.

AASHTO (1996), *Standard Specification for Highway Bridges*, Sixteenth Edition, Washington, D.C.

AASHTO (1998), *AASHTO LRFD Bridge Design Specifications*, Second Edition, Washington, D.C.

Schilling, C. G., Barker, M. G., Dishongh, B. E., and Hartnagel, B. A. (1997), *Inelastic Design Procedures and Specifications*, Final Report submitted to AISI for study on Development and Experimental Verification of Inelastic Design Procedures for Steel Bridges Comprising Noncompact Sections, January.

Hartnagel, B. A. (1997), *Inelastic Design and Experimental Testing of Compact and Noncompact Steel Girder Bridges*, Dissertation, University of Missouri – Columbia, Columbia, MO, August.

Schilling, C. G. (1991), "Unified Autostress Method," *Engineering Journal*, AISC, Vol. 28, No. 4, Fourth Quarter.

Schilling, C. G. (1993), "Unified Autostress Method," *Transportation Research Record 1380*, TRB, National Research Council, Washington, D.C.

Dishongh, B. E., and Galambos, T. V. (1992), "Residual Deflection Analysis for Inelastic Bridge Rating," *Journal of Structural Engineering*, ASCE, Vol. 118, No. 6., June.

Schilling, C. G., and Morcos, S. S. (1988), "Moment-Rotation Tests of Steel Girders with Ultracompact Flanges," *Report on Project 188*, AISI, July.